International Journal of Chemical and Biochemical Sciences
(ISSN 2226-9614)

Journal Home page: www.iscientific.org/Journal.html

Unveiling the Potential of Andrographolide Derivatives as PI3K Inhibitors Structural Optimization, Molecular Docking Insights, and *In-Vitro* Anti-Cancer Activity

Vishwanadham Yerragunta[1]*, Kavita Waghray[1], Shivraj[2], Appaji.D[3], NJP Subhashini[2]

[1]Department of Pharmacy, University College of Technology, Osmania University, Hyderabad 500007, Telangana, India.
[2]Department of Chemistry, University College of Science, Osmania University, Hyderabad 500007, Telangana, India.
[3]Dr. Reddy's Institute of Life Sciences, Centre for Innovation in Molecular and Pharmaceutical Sciences, Serilingampalle (M), Telangana 500046, India.

Abstract

Andrographolide, extracted from Andrographis paniculata, exhibits promising therapeutic properties against cancer and various diseases. This study focuses on the design and evaluation of novel andrographolide analogues inspired by structural activity relationships. The analogues underwent rigorous prediction of absorption, distribution, metabolism, and excretion (ADME) properties, followed by molecular docking studies against the PI3K inhibitor (PDB ID: 3ML8) using Schrödinger software (version 10.1). Our computational analysis revealed favorable binding affinities of the analogues towards the active site of the target protein. Notably, compounds 14, 11, and 9 demonstrated particularly strong binding interactions with the receptor. Subsequent MTT assays were conducted on diverse human cancer cell lines (MCF-7, HepG2, HT-116, PC3) to assess the cytotoxic potential of the analogues. Several compounds exhibited significant cytotoxicity, with IC50 values surpassing those of the standard drug, doxorubicin. These findings underscore the potential of andrographolide derivatives as promising candidates for cancer therapy, emphasizing the importance of rational drug design in the quest for novel anticancer agents.

Keywords: Andrographolide analogous, ADME, PI3K Inhibitor, Molecular docking, anti-cancer activity

Full length article **Corresponding Author*, e-mail: vishwanadham.y@gmail.com

1. Introduction

Andrographolide, a labdane diterpenoid isolated from the leaves of Andrographis paniculata (Acanthaceae), has garnered significant interest in the field of pharmacology due to its diverse pharmacological activities. As a major phytoconstituent, andrographolide exhibits potent anticancer properties by inducing apoptosis, a programmed cell death mechanism essential for maintaining tissue homeostasis and suppressing tumorigenesis [1-2]. In addition to its anticancer effects, andrographolide demonstrates a broad spectrum of pharmacological activities, including anti-viral, antimalarial, anti-inflammatory, immune stimulatory, and anti-hyperglycemic effects [3]. In recent years, the emergence of computer-aided drug design (CADD) has revolutionized the drug discovery and development process. The exponential growth of chemical and biological databases, coupled with the development of sophisticated software tools, has provided researchers with unprecedented opportunities to design ligands and inhibitors with enhanced specificity and efficacy [4]. CADD techniques encompass a wide range of computational methods, including molecular modeling, virtual screening, and molecular dynamics simulations, which enable the rapid and cost-effective identification of potential drug candidates [5]. The phosphoinositide 3-kinase (PI3K)-targeting signaling pathways have emerged as promising targets for cancer therapy. Dysregulation of PI3K signaling is frequently observed in human cancers, contributing to aberrant cell growth, survival, and metastasis [6-7]. The success of imatinib in treating chronic myeloid leukemia has validated the therapeutic potential of targeting specific signaling pathways in cancer treatment and has spurred the development of additional targeted therapies. To

date, numerous drugs targeting mutated proteins involved in cancer growth have been evaluated in clinical trials, underscoring the importance of targeted therapies in modern oncology [8-9].

2. Materials and Methods

Andrographolide analogous derived[10-14]. from the natural substituents were structural modification by changing the core structure and functional group. NMR, and MS were used to identify the structures of andrographolide analogues. After modifying the primary structure and functional groups of andrographolide, similar results were observed [15-21].

2.1. Scheme

General Synthetic scheme of new Andrographolides and Table 1.

2.2. Chemistry

Andrographolide: White solid, % yield 0.93 %; IR (Neat): 3194, 3096, 1648, 1402, 1168, 1021cm -1 ; 1H-NMR: (400 MHz): δ 6.84 (1H, td, J 06.0, 1.0Hz, H-12), 4.41 (1-H, d, J0 6.0 Hz, H-14), 4.08 (1-H, br, H 17b), 4.56 (1-H, brs, H-17 a), 4.32 (1-H, dd, J 010.0, 6.0 Hz, H-15b), 4.07 (1-H, dd, J0 10, 2- Hz, H-15a), 4.71 (1-H,d, J0 11.0 Hz, H-v19b), 3.68 (1-H, d, J0 11.0 Hz, H-19a), 3.25−3.14 (1-H, m), 2.59 −2.39 (2-H, m), 2.62 (1H, dt, J 07.0, 2.0 Hz), 1.96 −1.58 (5H, m), 1.36 − 1.14 (4-H, m), 1.14 (3-H, s, H-18), 0.58 (3-H, s, H-20); 13C NMR (100 MHz): δ172.71 (c-16), 148.82 (c-12), 147.64 (c-8), 128.63 (c-13), 198.84 (c-17), 80.94 (c-3), 76.19 (c-15), 66.64 (c-14), 57.38 (c-9), 56.32 (c-5), 43.68 (c-4), 38.96 (c-7), 38.13 (c-1), 29.00 (c-2), 24.73 (c-6), 25.20 (c-11), 23.27 (c-18), 15.58 (c-20)

1. ^{1}H NMR (500 MHz, Chloroform-*d*) δ 6.61 (tt, *J* = 7.3, 1.8 Hz, 1H), 4.82 (d, *J* = 1.0 Hz, 1H), 4.74 (d, *J* = 1.0 Hz, 2H), 3.89 – 3.18 (m, 7H), 2.93 – 2.58 (m, 5H), 2.54 – 2.46 (m, 1H), 2.44 – 2.37 (m, 2H), 2.15 – 0.63 (m, 17H).
^{13}C NMR (125 MHz, Common NMR Solvents) δ 210.69, 172.91, 161.37 (d, *J* = 246.4 Hz), 148.16, 136.36 (d, *J* = 3.6 Hz), 130.59 – 119.09 (m), 115.34 (d, *J* = 22.4 Hz), 83.85, 69.91 (d, *J* = 334.6 Hz), 60.26, 48.96 (d, *J* = 203.9 Hz), 44.79 – 41.56 (m), 40.93 – 35.66 (m), 33.06 – 28.01 (m), 23.29 – 14.78 (m).

2. ^{1}H NMR (500 MHz, Chloroform-*d*) δ 8.10 (t, *J* = 0.9 Hz, 1H), 7.62 (dd, *J* = 7.0, 1.4 Hz, 1H), 7.43 (dd, *J* = 5.9, 1.4 Hz, 1H), 7.36 – 7.30 (m, 1H), 7.20 – 7.11 (m, 3H), 7.06 – 6.99 (m, 2H), 6.61 (tt, *J* = 7.3, 1.8 Hz, 1H), 4.87 – 4.81 (m, 2H), 4.73 (dd, *J* = 13.5, 1.0 Hz, 1H), 3.89 – 3.81 (m, 3H), 3.81 – 3.74 (m, 1H), 3.66 – 3.52 (m, 2H), 3.32 (t, *J* = 6.0 Hz, 1H), 2.86 – 2.65 (m, 5H), 2.54 – 2.46 (m, 1H), 2.45 – 2.36 (m, 2H), 2.17 (dtd, *J* = 15.6, 7.4, 1.0 Hz, 1H), 1.86 (dddd, *J* = 14.0, 9.2, 6.6, 4.9 Hz, 1H), 1.67 – 1.43 (m, 6H), 1.42 – 1.19 (m, 4H), 1.04 (t, *J* = 1.5 Hz, 3H), 0.82 (t, *J* = 1.5 Hz, 3H).

^{13}C NMR (125 MHz, Common NMR Solvents) δ 210.69, 172.91, 162.35, 160.38, 149.74, 143.25, 136.37, 136.35, 135.33, 132.21, 131.83, 130.45, 130.38, 130.16, 128.15, 127.60, 119.60, 117.80, 115.43, 115.25, 83.85, 71.25, 68.57, 60.28, 49.78, 48.15, 44.08, 43.70, 43.04, 37.96, 37.47, 36.95, 31.56, 30.02, 28.97, 25.66, 25.44, 22.65, 18.92, 16.37.

3. ^{1}H NMR (500 MHz, Chloroform-*d*) δ 8.42 (d, *J* = 1.0 Hz, 2H), 7.62 (dd, *J* = 7.3, 1.4 Hz, 2H), 7.49 (td, *J* = 7.0, 1.4 Hz, 2H), 7.34 (td, *J* = 7.2, 1.1 Hz, 2H), 7.29 – 7.24 (m, 2H), 7.14 (ddt, *J* = 8.1, 3.5, 0.8 Hz, 4H), 7.06 – 6.99 (m, 4H), 6.61 (tt, *J* = 7.3, 1.8 Hz, 2H), 4.84 (dd, *J* = 13.6, 0.8 Hz, 2H), 4.73 (dd, *J* = 13.5, 1.0 Hz, 2H), 3.89 – 3.81 (m, 6H), 3.81 – 3.78 (m, 1H), 3.76 (dq, *J* = 4.9, 1.5 Hz, 2H), 3.66 – 3.52 (m, 4H), 3.32 (t, *J* = 6.0 Hz, 2H), 2.86 – 2.78 (m, 5H), 2.78 – 2.70 (m, 5H), 2.70 – 2.65 (m, 1H), 2.54 – 2.46 (m, 2H), 2.45 – 2.36 (m, 4H), 2.17 (dtd, *J* = 15.6, 7.4, 1.0 Hz, 2H), 1.86 (dddd, *J* = 14.0, 9.2, 6.6, 4.9 Hz, 2H), 1.67 – 1.58 (m, 3H), 1.58 – 1.54 (m, 2H), 1.54 – 1.48 (m, 5H), 1.48 – 1.43 (m, 2H), 1.42 – 1.19 (m, 8H), 1.04 (t, *J* = 1.5 Hz, 6H), 0.82 (t, *J* = 1.5 Hz, 6H).

^{13}C NMR (125 MHz, Common NMR Solvents) δ 210.69, 172.91, 162.35, 160.38, 149.32, 143.25, 136.73, 136.36 (d, *J* = 3.6 Hz), 132.76, 132.21, 131.01, 130.41 (d, *J* = 8.6 Hz), 128.58, 127.46, 120.67, 118.71, 115.43, 115.25, 83.85, 71.25, 68.57, 60.28, 49.78, 48.15, 44.08, 43.70, 43.04, 37.96, 37.47, 36.95, 31.56, 30.02, 28.97, 25.66, 25.44, 22.65, 18.92, 17.49, 16.37.

4. ^{1}H NMR (500 MHz, Chloroform-*d*) δ 8.28 (t, *J* = 0.8 Hz, 1H), 7.62 (dd, *J* = 7.3, 1.4 Hz, 1H), 7.35 (td, *J* = 7.2, 1.2 Hz, 1H), 7.20 (td, *J* = 7.1, 1.4 Hz, 1H), 7.17 – 7.11 (m, 2H), 7.06 – 6.99 (m, 3H), 6.61 (tt, *J* = 7.3, 1.8 Hz, 1H), 4.87 – 4.80 (m, 1H), 4.73 (dd, *J* = 13.5, 1.0 Hz, 1H), 3.91 – 3.80 (m, 6H), 3.80 – 3.74 (m, 1H), 3.66 – 3.52 (m, 2H), 3.32 (t, *J* = 5.9 Hz, 1H), 2.86 – 2.65 (m, 5H), 2.50 (dd, *J* = 15.4, 7.7 Hz, 1H), 2.45 – 2.36 (m, 2H), 2.17 (dtd, *J* = 15.6, 7.4, 1.0 Hz, 1H), 1.86 (dddd, *J* = 13.9, 9.1, 6.6, 4.9 Hz, 1H), 1.67 – 1.43 (m, 6H), 1.42 – 1.19 (m, 4H), 1.04 (t, *J* = 1.5 Hz, 3H), 0.82 (t, *J* = 1.6 Hz, 3H).

^{13}C NMR (125 MHz, Common NMR Solvents) δ 176.66 – 105.21 (m), 40.13 – 14.92 (m).

^{13}C NMR (125 MHz, Common NMR Solvents) δ 210.69, 172.91, 162.35, 160.38, 153.87, 148.29, 143.25, 136.37, 136.35, 132.21, 130.45, 130.38, 127.25, 126.87, 124.88, 119.76, 119.72, 115.43, 115.25, 114.05, 83.85, 71.25, 68.57, 60.26, 55.72, 49.78, 48.15, 44.08, 43.70, 43.04, 37.96, 37.47, 36.95, 31.56, 30.02, 28.97, 25.66, 25.44, 22.65, 18.92, 16.37.

5. ^{1}H NMR (500 MHz, Chloroform-*d*) δ 8.28 (t, *J* = 0.9 Hz, 1H), 7.64 (dd, *J* = 7.3, 1.4 Hz, 1H), 7.35 (td, *J* = 7.2, 1.2 Hz, 1H), 7.21 (td, *J* = 7.1, 1.4 Hz, 1H), 7.15 (ddt, *J* = 8.2, 3.5, 0.9 Hz, 2H), 7.06 – 6.96 (m, 3H), 6.61 (tt, *J* = 7.3, 1.8 Hz, 1H), 4.87 – 4.80 (m, 1H), 4.73 (dd, *J* = 13.5, 1.0 Hz, 1H), 4.11 (q, *J* = 6.2 Hz, 2H), 3.89 – 3.81 (m, 3H), 3.81 – 3.74 (m, 1H), 3.66 – 3.52 (m, 2H), 3.32 (t, *J* = 6.0 Hz, 1H), 2.86 – 2.65 (m, 5H), 2.54 – 2.46 (m, 1H), 2.45 – 2.36 (m, 2H), 2.17 (dtd, *J* = 15.6, 7.4, 1.0 Hz, 1H), 1.86 (dddd, *J* = 14.0, 9.2, 6.6, 4.9 Hz, 1H), 1.67 – 1.19 (m, 13H), 1.04 (t, *J* = 1.4 Hz, 3H), 0.82 (t, *J* = 1.5 Hz, 3H).

^{13}C NMR (125 MHz, Common NMR Solvents) δ 210.69, 172.91, 162.35, 160.38, 152.38, 148.31, 143.25, 136.36 (d, *J* = 3.6 Hz), 132.21, 130.41 (d, *J* = 8.6 Hz), 126.59 (d, *J* = 2.1 Hz), 124.94, 120.09, 119.84, 115.43, 115.25, 115.09, 83.85,

71.25, 68.57, 64.69, 60.26, 49.78, 48.15, 44.08, 43.70, 43.04, 37.96, 37.47, 36.95, 31.56, 30.02, 28.97, 25.66, 25.44, 22.65, 18.92, 16.37, 14.91.

6. ^{1}***H NMR*** (500 MHz, Chloroform-*d*) δ 9.12 (t, *J* = 0.9 Hz, 1H), 8.29 (dd, *J* = 7.9, 1.4 Hz, 1H), 7.89 (dd, *J* = 6.8, 1.3 Hz, 1H), 7.70 (td, *J* = 6.9, 1.5 Hz, 1H), 7.43 (ddd, *J* = 7.9, 6.6, 1.3 Hz, 1H), 7.18 – 7.11 (m, 2H), 7.06 – 6.99 (m, 2H), 6.61 (tt, *J* = 7.3, 1.8 Hz, 1H), 4.84 (dd, *J* = 13.5, 0.7 Hz, 1H), 4.73 (dd, *J* = 13.6, 0.9 Hz, 1H), 3.89 – 3.81 (m, 3H), 3.81 – 3.74 (m, 1H), 3.66 – 3.52 (m, 2H), 3.32 (t, *J* = 6.0 Hz, 1H), 2.86 – 2.79 (m, 2H), 2.79 – 2.65 (m, 3H), 2.50 (dd, *J* = 15.4, 7.7 Hz, 1H), 2.45 – 2.36 (m, 2H), 2.17 (dtd, *J* = 15.6, 7.4, 1.0 Hz, 1H), 1.86 (dddd, *J* = 13.9, 9.2, 6.6, 4.9 Hz, 1H), 1.67 – 1.58 (m, 1H), 1.58 – 1.54 (m, 1H), 1.54 – 1.48 (m, 2H), 1.48 – 1.44 (m, 1H), 1.42 – 1.19 (m, 4H), 1.04 (t, *J* = 1.4 Hz, 3H), 0.82 (t, *J* = 1.5 Hz, 3H).

^{13}C NMR (125 MHz, Common NMR Solvents) δ 210.69, 172.91, 162.35, 160.38, 148.86, 143.25, 142.78, 136.37, 136.35, 133.13, 132.21, 131.09, 130.45, 130.38, 127.54, 127.50, 121.10, 118.16, 115.43, 115.25, 83.85, 71.25, 68.57, 60.24, 49.78, 48.15, 44.08, 43.70, 43.04, 37.96, 37.47, 36.95, 31.56, 30.02, 28.97, 25.66, 25.44, 22.65, 18.92, 16.37.

7. ^{1}***H NMR*** (500 MHz, Chloroform-*d*) δ 8.52 (t, *J* = 0.9 Hz, 2H), 7.75 (t, *J* = 2.1 Hz, 2H), 7.63 (ddd, *J* = 8.1, 2.1, 1.0 Hz, 2H), 7.44 (t, *J* = 8.1 Hz, 2H), 7.21 – 7.11 (m, 6H), 7.06 – 6.99 (m, 4H), 6.61 (tt, *J* = 7.3, 1.8 Hz, 2H), 4.84 (dd, *J* = 13.6, 0.8 Hz, 2H), 4.73 (dd, *J* = 13.5, 1.0 Hz, 2H), 3.89 – 3.81 (m, 6H), 3.81 – 3.78 (m, 1H), 3.78 – 3.74 (m, 2H), 3.66 – 3.52 (m, 4H), 3.32 (t, *J* = 6.0 Hz, 2H), 2.86 – 2.78 (m, 5H), 2.78 – 2.70 (m, 5H), 2.70 – 2.65 (m, 1H), 2.54 – 2.46 (m, 2H), 2.45 – 2.36 (m, 4H), 2.17 (dtd, *J* = 15.6, 7.4, 1.0 Hz, 2H), 1.86 (dddd, *J* = 14.0, 9.2, 6.6, 4.9 Hz, 2H), 1.67 – 1.58 (m, 3H), 1.58 – 1.54 (m, 2H), 1.54 – 1.48 (m, 5H), 1.48 – 1.43 (m, 2H), 1.42 – 1.19 (m, 8H), 1.04 (t, *J* = 1.4 Hz, 6H), 0.82 (t, *J* = 1.5 Hz, 6H).

^{13}C NMR (125 MHz, Common NMR Solvents) δ 210.69, 172.91, 170.52 – 149.33 (m), 143.25, 141.36 – 133.71 (m), 132.21, 131.33, 130.41 (d, *J* = 8.6 Hz), 126.76, 119.99, 118.84, 117.86, 115.43, 115.25, 83.85, 71.25, 68.57, 60.13, 49.78, 48.15, 44.08, 43.70, 43.04, 37.96, 37.47, 36.95, 31.56, 30.02, 28.97, 25.66, 25.44, 22.65, 18.92, 16.37.

8. ^{1}***H NMR*** (500 MHz, Chloroform-*d*) δ 8.55 (t, *J* = 0.9 Hz, 1H), 7.72 (q, *J* = 1.4 Hz, 1H), 7.68 – 7.60 (m, 1H), 7.32 – 7.25 (m, 2H), 7.14 (ddt, *J* = 8.1, 3.5, 0.8 Hz, 2H), 7.06 – 6.99 (m, 2H), 6.61 (tt, *J* = 7.3, 1.8 Hz, 1H), 4.84 (dd, *J* = 13.6, 0.8 Hz, 1H), 4.73 (dd, *J* = 13.5, 1.0 Hz, 1H), 3.89 – 3.81 (m, 3H), 3.81 – 3.74 (m, 1H), 3.66 – 3.52 (m, 2H), 3.32 (t, *J* = 6.0 Hz, 1H), 2.86 – 2.65 (m, 5H), 2.54 – 2.46 (m, 1H), 2.45 – 2.36 (m, 2H), 2.17 (dtd, *J* = 15.6, 7.4, 1.0 Hz, 1H), 1.86 (dddd, *J* = 14.0, 9.2, 6.6, 4.9 Hz, 1H), 1.67 – 1.54 (m, 2H), 1.54 – 1.48 (m, 3H), 1.48 – 1.43 (m, 1H), 1.42 – 1.19 (m, 4H), 1.04 (t, *J* = 1.5 Hz, 3H), 0.82 (t, *J* = 1.5 Hz, 3H).

^{13}C NMR (125 MHz, Common NMR Solvents) δ 210.69, 172.91, 162.35, 160.38, 149.75, 143.25, 137.35, 136.36 (d, *J* = 3.6 Hz), 132.21, 130.41 (d, *J* = 8.6 Hz), 129.28, 123.37, 123.00, 118.92, 117.64, 115.43, 115.25, 83.85, 71.25, 68.57, 60.13, 49.78, 48.15, 44.08, 43.70, 43.04, 37.96, 37.47, 36.95, 31.56, 30.02, 28.97, 25.66, 25.44, 22.65, 18.92, 16.37.

9. ^{1}***H NMR*** (500 MHz, Chloroform-*d*) δ 8.55 (t, *J* = 0.8 Hz, 1H), 8.22 (t, *J* = 2.1 Hz, 1H), 7.84 (ddd, *J* = 7.5, 2.2, 1.3 Hz, 1H), 7.77 (ddd, *J* = 7.5, 2.1, 1.2 Hz, 1H), 7.61 (t, *J* = 7.4 Hz, 1H), 7.18 – 7.11 (m, 2H), 7.06 – 6.99 (m, 2H), 6.61 (tt, *J* = 7.3, 1.8 Hz, 1H), 4.84 (dd, *J* = 13.6, 0.8 Hz, 1H), 4.73 (dd, *J* = 13.6, 0.9 Hz, 1H), 3.89 – 3.81 (m, 3H), 3.81 – 3.74 (m, 1H), 3.63 (dd, *J* = 11.3, 5.9 Hz, 1H), 3.60 – 3.52 (m, 1H), 3.32 (t, *J* = 5.9 Hz, 1H), 2.87 – 2.65 (m, 5H), 2.62 (s, 3H), 2.50 (dd, *J* = 15.4, 7.7 Hz, 1H), 2.45 – 2.36 (m, 2H), 2.17 (dtd, *J* = 15.6, 7.3, 1.0 Hz, 1H), 1.86 (dddd, *J* = 13.9, 9.2, 6.6, 4.9 Hz, 1H), 1.67 – 1.43 (m, 6H), 1.42 – 1.19 (m, 4H), 1.04 (t, *J* = 1.5 Hz, 3H), 0.82 (t, *J* = 1.6 Hz, 3H).

^{13}C NMR (125 MHz, Common NMR Solvents) δ 210.69, 197.50, 172.91, 162.35, 160.38, 149.77, 143.25, 138.23, 137.61, 136.37, 136.35, 132.21, 130.45, 130.38, 129.84, 126.18, 122.13, 119.43, 118.88, 115.43, 115.25, 83.85, 71.25, 68.57, 60.13, 49.78, 48.15, 44.08, 43.70, 43.04, 37.96, 37.47, 36.95, 31.56, 30.02, 28.97, 26.70, 25.66, 25.44, 22.65, 18.92, 16.37.

10. ^{1}***H NMR*** (500 MHz, Chloroform-*d*) δ 8.52 (t, *J* = 0.9 Hz, 1H), 7.96 (dt, *J* = 2.1, 1.1 Hz, 1H), 7.65 – 7.61 (m, 1H), 7.61 – 7.52 (m, 2H), 7.18 – 7.11 (m, 2H), 7.06 – 6.99 (m, 2H), 6.61 (tt, *J* = 7.3, 1.8 Hz, 1H), 4.84 (dd, *J* = 13.6, 0.8 Hz, 1H), 4.73 (dd, *J* = 13.5, 1.0 Hz, 1H), 3.89 – 3.81 (m, 3H), 3.81 – 3.74 (m, 1H), 3.66 – 3.52 (m, 2H), 3.32 (t, *J* = 6.0 Hz, 1H), 2.86 – 2.65 (m, 5H), 2.54 – 2.46 (m, 1H), 2.45 – 2.36 (m, 2H), 2.17 (dtd, *J* = 15.6, 7.4, 1.0 Hz, 1H), 1.86 (dddd, *J* = 14.0, 9.2, 6.6, 4.9 Hz, 1H), 1.67 – 1.58 (m, 1H), 1.58 – 1.54 (m, 1H), 1.54 – 1.48 (m, 2H), 1.48 – 1.43 (m, 1H), 1.42 – 1.19 (m, 4H), 1.04 (t, *J* = 1.5 Hz, 3H), 0.82 (t, *J* = 1.5 Hz, 3H).

^{13}C NMR (125 MHz, Common NMR Solvents) δ 210.70, 172.91, 162.35, 160.38, 149.71, 143.25, 136.47 – 136.14 (m), 132.21, 130.41 (d, *J* = 8.6 Hz), 129.94 (q, *J* = 3.6 Hz), 123.12 – 122.79 (m), 119.66 – 119.36 (m), 118.67, 115.43, 115.25, 83.85, 71.25, 68.57, 60.13, 49.78, 48.15, 44.08, 43.70, 43.04, 37.96, 37.47, 36.95, 31.56, 30.02, 28.97, 25.66, 25.44, 22.65, 18.92, 16.37.

11. ^{1}***H NMR*** (500 MHz, Chloroform-*d*) δ 8.50 (t, *J* = 0.9 Hz, 1H), 8.25 (s, 1H), 7.57 – 7.51 (m, 2H), 7.18 – 7.11 (m, 2H), 7.06 – 6.99 (m, 2H), 6.98 – 6.92 (m, 2H), 6.61 (tt, *J* = 7.3, 1.8 Hz, 1H), 4.84 (dd, *J* = 13.6, 0.8 Hz, 1H), 4.73 (dd, *J* = 13.5, 1.0 Hz, 1H), 3.89 – 3.81 (m, 3H), 3.81 – 3.74 (m, 1H), 3.66 – 3.52 (m, 2H), 3.32 (t, *J* = 6.0 Hz, 1H), 2.86 – 2.65 (m, 5H), 2.54 – 2.46 (m, 1H), 2.45 – 2.36 (m, 2H), 2.17 (dtd, *J* = 15.6, 7.4, 1.0 Hz, 1H), 1.86 (dddd, *J* = 14.0, 9.2, 6.6, 4.9 Hz, 1H), 1.67 – 1.54 (m, 2H), 1.54 – 1.48 (m, 3H), 1.48 – 1.43 (m, 1H), 1.42 – 1.19 (m, 4H), 1.04 (t, *J* = 1.4 Hz, 3H), 0.82 (t, *J* = 1.5 Hz, 3H).

^{13}C NMR (125 MHz, Common NMR Solvents) δ 210.69, 172.91, 162.35, 160.38, 156.79, 149.74, 143.25, 136.36 (d, *J* = 3.6 Hz), 132.21, 130.41 (d, *J* = 8.6 Hz), 129.74, 122.06, 118.58, 117.42, 115.43, 115.25, 83.85, 71.25, 68.57, 60.13, 49.78, 48.15, 44.08, 43.70, 43.04, 37.96, 37.47, 36.95, 31.56, 30.02, 28.97, 25.66, 25.44, 22.65, 18.92, 16.37.

12. ^{1}***H NMR*** (500 MHz, Chloroform-*d*) δ 8.48 (t, *J* = 0.8 Hz, 1H), 7.59 – 7.53 (m, 2H), 7.44 – 7.39 (m, 2H), 7.18 – 7.11

(m, 2H), 7.06 – 6.99 (m, 2H), 6.61 (tt, *J* = 7.3, 1.8 Hz, 1H), 4.84 (dd, *J* = 13.6, 0.8 Hz, 1H), 4.73 (dd, *J* = 13.5, 1.0 Hz, 1H), 4.27 (s, 1H), 3.89 – 3.81 (m, 3H), 3.81 – 3.74 (m, 1H), 3.66 – 3.52 (m, 2H), 3.32 (t, *J* = 6.0 Hz, 1H), 2.86 – 2.65 (m, 5H), 2.54 – 2.46 (m, 1H), 2.45 – 2.36 (m, 2H), 2.17 (dtd, *J* = 15.6, 7.4, 1.0 Hz, 1H), 1.86 (dddd, *J* = 14.0, 9.2, 6.6, 4.9 Hz, 1H), 1.67 – 1.58 (m, 1H), 1.58 – 1.54 (m, 1H), 1.54 – 1.50 (m, 2H), 1.50 – 1.43 (m, 2H), 1.42 – 1.19 (m, 4H), 1.04 (t, *J* = 1.4 Hz, 3H), 0.82 (t, *J* = 1.5 Hz, 3H).

^{13}C NMR (125 MHz, Common NMR Solvents) δ 210.69, 172.91, 169.46 – 149.56 (m), 143.25, 136.36 (d, *J* = 3.6 Hz), 133.97, 132.21, 131.43, 131.19, 130.41 (d, *J* = 8.6 Hz), 120.44, 118.55, 115.43, 115.25, 83.85, 71.25, 68.57, 60.13, 49.78, 48.15, 44.08, 43.70, 43.04, 37.96, 37.47, 36.95, 31.56, 30.02, 28.97, 25.66, 25.44, 22.65, 18.92, 16.37.

13. ^{1}H NMR (500 MHz, Chloroform-*d*) δ 8.51 (d, *J* = 1.0 Hz, 1H), 7.69 – 7.63 (m, 2H), 7.28 (dd, *J* = 8.8, 0.9 Hz, 2H), 7.14 (ddt, *J* = 8.1, 3.5, 0.8 Hz, 2H), 7.06 – 6.99 (m, 2H), 6.61 (tt, *J* = 7.3, 1.8 Hz, 1H), 4.84 (dd, *J* = 13.6, 0.8 Hz, 1H), 4.73 (dd, *J* = 13.5, 1.0 Hz, 1H), 3.89 – 3.81 (m, 3H), 3.81 – 3.74 (m, 1H), 3.66 – 3.52 (m, 2H), 3.32 (t, *J* = 6.0 Hz, 1H), 2.86 – 2.65 (m, 5H), 2.54 – 2.46 (m, 1H), 2.45 – 2.36 (m, 5H), 2.17 (dtd, *J* = 15.6, 7.4, 1.0 Hz, 1H), 1.86 (dddd, *J* = 13.9, 9.2, 6.6, 4.9 Hz, 1H), 1.67 – 1.59 (m, 1H), 1.59 – 1.49 (m, 3H), 1.49 – 1.43 (m, 2H), 1.42 – 1.19 (m, 4H), 1.04 (t, *J* = 1.5 Hz, 3H), 0.82 (t, *J* = 1.5 Hz, 3H).

^{13}C NMR (125 MHz, Common NMR Solvents) δ 143.96 – 93.54 (m).

^{13}C NMR (125 MHz, Common NMR Solvents) δ 210.69, 172.91, 162.35, 160.38, 149.73, 143.25, 137.18, 136.37, 136.35, 134.73, 132.21, 130.53, 130.45, 130.38, 120.32, 118.76, 115.43, 115.25, 83.85, 71.25, 68.57, 60.13, 49.78, 48.15, 44.08, 43.70, 43.04, 37.96, 37.47, 36.95, 31.56, 30.02, 28.97, 25.66, 25.44, 22.65, 21.07, 18.92, 16.37.

14. ^{1}H NMR (500 MHz, Chloroform-*d*) δ 8.49 (t, *J* = 0.8 Hz, 1H), 7.63 – 7.57 (m, 2H), 7.18 – 7.11 (m, 2H), 7.06 – 6.97 (m, 4H), 6.61 (tt, *J* = 7.3, 1.8 Hz, 1H), 4.84 (dd, *J* = 13.6, 0.8 Hz, 1H), 4.73 (dd, *J* = 13.5, 0.9 Hz, 1H), 3.89 – 3.81 (m, 3H), 3.80 (s, 3H), 3.80 – 3.74 (m, 4H), 3.66 – 3.52 (m, 2H), 3.32 (t, *J* = 5.9 Hz, 1H), 2.86 – 2.65 (m, 5H), 2.50 (dd, *J* = 15.4, 7.7 Hz, 1H), 2.45 – 2.36 (m, 2H), 2.17 (dtd, *J* = 15.6, 7.4, 1.0 Hz, 1H), 1.86 (dddd, *J* = 13.9, 9.2, 6.6, 4.9 Hz, 1H), 1.67 – 1.43 (m, 6H), 1.42 – 1.19 (m, 4H), 1.04 (t, *J* = 1.5 Hz, 3H), 0.82 (t, *J* = 1.6 Hz, 3H).

^{13}C NMR (125 MHz, Common NMR Solvents) δ 210.69, 172.91, 162.35, 160.38, 159.88, 149.74, 143.25, 136.36 (d, *J* = 3.6 Hz), 132.21, 130.82, 130.41 (d, *J* = 8.6 Hz), 122.13, 118.58, 115.34 (t, *J* = 11.2 Hz), 83.85, 71.25, 68.57, 60.13, 55.35, 49.78, 48.15, 44.08, 43.70, 43.04, 37.96, 37.47, 36.95, 31.56, 30.02, 28.97, 25.66, 25.44, 22.65, 18.92, 16.37.

15. ^{1}H NMR (500 MHz, Chloroform-*d*) δ 8.49 (d, *J* = 0.9 Hz, 1H), 7.66 – 7.60 (m, 2H), 7.18 – 7.11 (m, 2H), 7.06 – 7.01 (m, 2H), 7.01 – 6.97 (m, 2H), 6.61 (tt, *J* = 7.3, 1.8 Hz, 1H), 4.84 (dd, *J* = 13.6, 0.8 Hz, 1H), 4.73 (dd, *J* = 13.5, 1.0 Hz, 1H), 4.03 (q, *J* = 6.7 Hz, 2H), 3.89 – 3.81 (m, 3H), 3.81 – 3.74 (m, 1H), 3.66 – 3.52 (m, 2H), 3.32 (t, *J* = 6.0 Hz, 1H), 2.86 – 2.65 (m, 5H), 2.54 – 2.46 (m, 1H), 2.45 – 2.36 (m, 2H), 2.17 (dtd, *J* = 15.6, 7.4, 1.0 Hz, 1H), 1.86 (dddd, *J* = 13.9, 9.2, 6.6, 4.9 Hz, 1H), 1.67 – 1.19 (m, 13H), 1.04 (t, *J* = 1.4 Hz, 3H), 0.82 (t, *J* = 1.5 Hz, 3H).

^{13}C NMR (125 MHz, Common NMR Solvents) δ 210.69, 172.91, 162.35, 160.38, 157.94, 149.74, 143.25, 136.36 (d, *J* = 3.6 Hz), 132.21, 131.37, 130.41 (d, *J* = 8.6 Hz), 122.51, 118.58, 117.20, 115.43, 115.25, 83.85, 71.25, 68.57, 63.57, 60.13, 49.78, 48.15, 44.08, 43.70, 43.04, 37.96, 37.47, 36.95, 31.56, 30.02, 28.97, 25.66, 25.44, 22.65, 18.92, 16.37, 14.69. 16F

16. ^{1}H NMR (500 MHz, Chloroform-*d*) δ 8.30 (t, *J* = 0.9 Hz, 1H), 8.23 (dd, *J* = 9.3, 2.2 Hz, 1H), 8.01 (d, *J* = 9.4 Hz, 1H), 7.87 (d, *J* = 2.1 Hz, 1H), 7.18 – 7.11 (m, 2H), 7.06 – 6.99 (m, 2H), 6.61 (tt, *J* = 7.3, 1.8 Hz, 1H), 4.87 – 4.80 (m, 1H), 4.73 (dd, *J* = 13.5, 1.0 Hz, 1H), 3.92 – 3.80 (m, 6H), 3.80 – 3.74 (m, 1H), 3.66 – 3.52 (m, 2H), 3.32 (t, *J* = 5.9 Hz, 1H), 2.86 – 2.65 (m, 5H), 2.50 (dd, *J* = 15.4, 7.7 Hz, 1H), 2.45 – 2.36 (m, 2H), 2.17 (dtd, *J* = 15.6, 7.4, 1.0 Hz, 1H), 1.86 (dddd, *J* = 13.9, 9.2, 6.6, 4.9 Hz, 1H), 1.67 – 1.43 (m, 6H), 1.42 – 1.19 (m, 4H), 1.04 (t, *J* = 1.5 Hz, 3H), 0.82 (t, *J* = 1.6 Hz, 3H).

^{13}C NMR (125 MHz, Common NMR Solvents) δ 210.69, 172.91, 162.35, 160.38, 153.72, 148.44, 145.95, 143.25, 136.36 (d, *J* = 3.6 Hz), 132.21, 131.84, 130.41 (d, *J* = 8.6 Hz), 119.93 (d, *J* = 3.3 Hz), 119.03, 115.43, 115.25, 108.54, 83.85, 71.25, 68.57, 60.28, 56.18, 49.78, 48.15, 44.08, 43.70, 43.04, 37.96, 37.47, 36.95, 31.56, 30.02, 28.97, 25.66, 25.44, 22.65, 18.92, 16.37.

17. ^{1}H NMR (500 MHz, Chloroform-*d*) δ 9.05 (t, *J* = 0.9 Hz, 2H), 7.90 (d, *J* = 8.7 Hz, 2H), 7.51 (d, *J* = 2.1 Hz, 2H), 7.32 (dd, *J* = 8.6, 2.2 Hz, 2H), 7.18 – 7.11 (m, 4H), 7.06 – 6.99 (m, 4H), 6.61 (tt, *J* = 7.3, 1.8 Hz, 2H), 4.84 (dd, *J* = 13.5, 0.7 Hz, 2H), 4.73 (dd, *J* = 13.5, 1.0 Hz, 2H), 3.89 – 3.74 (m, 14H), 3.66 – 3.52 (m, 4H), 3.32 (t, *J* = 5.9 Hz, 2H), 2.86 – 2.79 (m, 4H), 2.79 – 2.70 (m, 5H), 2.70 – 2.65 (m, 1H), 2.50 (dd, *J* = 15.4, 7.7 Hz, 2H), 2.45 – 2.36 (m, 4H), 2.17 (dtd, *J* = 15.6, 7.4, 1.0 Hz, 2H), 1.86 (dddd, *J* = 13.9, 9.2, 6.6, 4.9 Hz, 2H), 1.67 – 1.43 (m, 12H), 1.42 – 1.19 (m, 8H), 1.04 (t, *J* = 1.5 Hz, 6H), 0.82 (t, *J* = 1.6 Hz, 6H).

^{13}C NMR (125 MHz, Common NMR Solvents) δ 211.19, 172.57, 162.64, 160.67, 158.81, 144.84, 142.02, 141.72, 136.53 (d, *J* = 3.8 Hz), 132.05, 130.47 (d, *J* = 8.6 Hz), 126.72, 121.38, 120.26, 119.55, 115.43, 115.25, 111.77, 83.49, 71.97, 69.80, 60.94, 55.91, 50.24, 47.64, 44.17, 43.83, 43.00, 37.69, 36.76, 34.98, 31.38, 29.82, 29.20, 25.46 (d, *J* = 15.0 Hz), 23.39, 20.48, 16.36.

2.3. ADME analysis prediction

In drug discovery, understanding the absorption, distribution, metabolism, and excretion (ADME) properties of candidate compounds is crucial for optimizing their pharmacokinetic profile and ensuring their efficacy and safety. To assess the drug-likeness properties of the structurally modified compounds in our study, we employed the QikProp module within Schrödinger software 2017 for ADME prediction analysis. This computational approach allows for the rapid evaluation of various ADME parameters,

including molecular weight, lipophilicity, hydrogen bond donors and acceptors, and predicted oral absorption. Our analysis revealed that all the compounds exhibited favorable ADME profiles, with parameters falling within acceptable ranges for drug-like molecules. Specifically, the compounds demonstrated satisfactory percentages of human oral absorption, indicating their potential for effective oral administration. These findings are encouraging and suggest that the structurally modified compounds possess desirable pharmacokinetic properties, which are essential for their further development as potential therapeutic agents. The successful prediction of favorable ADME properties underscores the importance of employing computational tools in the early stages of drug discovery to guide the selection and optimization of candidate compounds. By leveraging predictive models and virtual screening techniques, researchers can prioritize compounds with the highest likelihood of success and minimize the resources expended on less promising candidates. Overall, the assessment of ADME properties represents a critical step in the rational design and optimization of novel drug candidates, ultimately facilitating the development of safer and more efficacious therapies for various diseases, including cancer. The calculated ADME properties for the andrographolide analogous compounds are tabulated Table 2.

Docking

The structures (ligands) were sketched in ChemDraw Ulta. All the ligands energy minimized and converted in to 3-Dimentional structures used by the ligprep tool using Schrodinger software 11.4. for the in-silico docking studies. All ligands were docked individually. Initially, the converted .mol molecule was loaded, and were set and saved in PDB. All the hetero atoms and water were removed in the 3ML8. PDB (Discovery of the Highly Potent PI3K/mTOR Inhibitor PF-04691502 through SBDD).

2.4. Cytotoxic Activity

HepG2, MCF-7, HCT 116, and PC3 cells were cultured in appropriate growth media and seeded onto a 96-well plate. After 24 hours of seeding, test samples at various concentrations were added to the wells, with a final volume of 20 µL of culture medium per well. The cells were then incubated for 72 hours at 37°C in a humidified atmosphere with 5% CO2. compounds. Subsequently, 15 µL of MTT (3-(4,5-dimethylthiazol-2-yl)-2,5-diphenyltetrazolium bromide) reagent, prepared in PBS to achieve a final concentration of 0.5 mg/mL, was added to each well. The plate was then incubated at 37°C for an additional 3 hours to allow the viable cells to metabolize the MTT dye. After the incubation period, the MTT reagent was carefully aspirated, and 100 µL of dimethyl sulfoxide (DMSO) was added to each well to solubilize the formazan crystals mixed on an orbital shaker for one hour at room temperature to ensure complete solubilization of the formazan crystals. Finally, the absorbance of the formazan solution in each well was measured at 570 nm using a microplate reader. The absorbance values obtained were proportional to the number of viable cells in each well, allowing for the assessment of cell viability and cytotoxicity induced by the test compounds.

3. Results and discussion

3.1. ADME toxicity properties prediction

We analyzed 18 andrographolide analogues, focusing on key molecular properties such as molecular weight, log Kp, logP, log P, MDCK permeability, and human absorption, in accordance with Lipinski's Rule of Five. Lipinski's Rule of Five serves as a guideline to assess drug likeness, aiding in the determination of whether a synthetic compound possesses characteristics conducive to becoming a viable oral drug candidate in humans. This rule delineates molecular features crucial for a drug's pharmacokinetics, particularly its absorption, distribution, metabolism, and excretion (ADME) properties. To evaluate the drug-like behavior of these compounds, we employed QikProp and Schrödinger software for the analysis of pharmacokinetic parameters necessary for ADME assessment. Among the 18 compounds tested, partition coefficient (QPlogPo/w) and water solubility (QPlogS) were of particular interest. The partition coefficient reflects the compound's ability to partition between octanol and water, influencing its absorption and distribution within the body. Meanwhile, water solubility is a critical determinant of a compound's bioavailability and can impact its pharmacokinetic behavior. Our analysis revealed a range of values for QPlogPo/w (5.203 to 7.523) and QPlogS (-5.383 to -9.463) among the tested compounds. These parameters play a pivotal role in predicting drug absorption and distribution characteristics, providing valuable insights into the pharmacokinetic behavior of the andrographolide analogues. By systematically evaluating these pharmacokinetic parameters, we can prioritize compounds with optimal drug-like properties for further development as potential therapeutic agents. An important component influencing drug metabolism and availability is cell permeability (QPPCaCO) 533.56.

3.2. Docking

The structures of the ligands were sketched using ChemDraw Ultra and subsequently energy-minimized and converted into 3-dimensional structures using the LigPrep tool within Schrödinger software version 11.4 for in-silico docking studies.

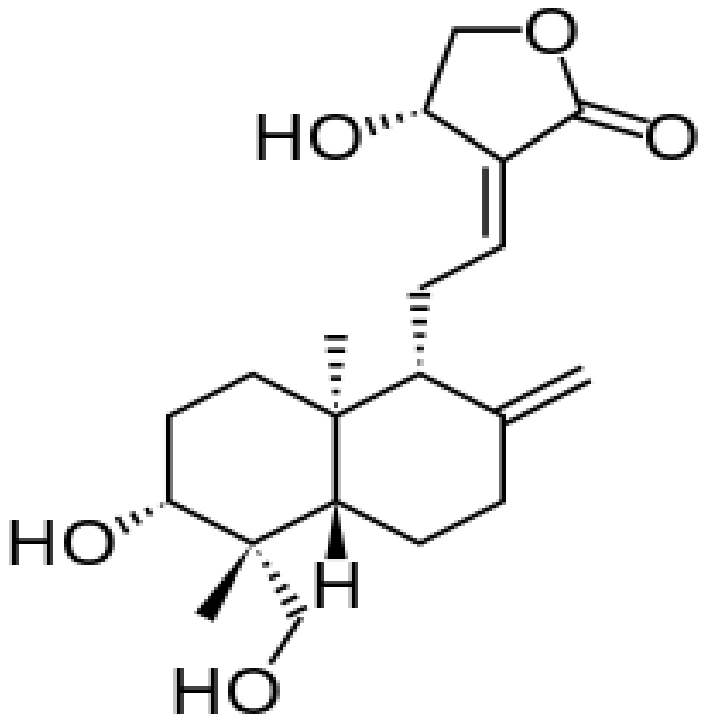

Figure 1. Andrographolide

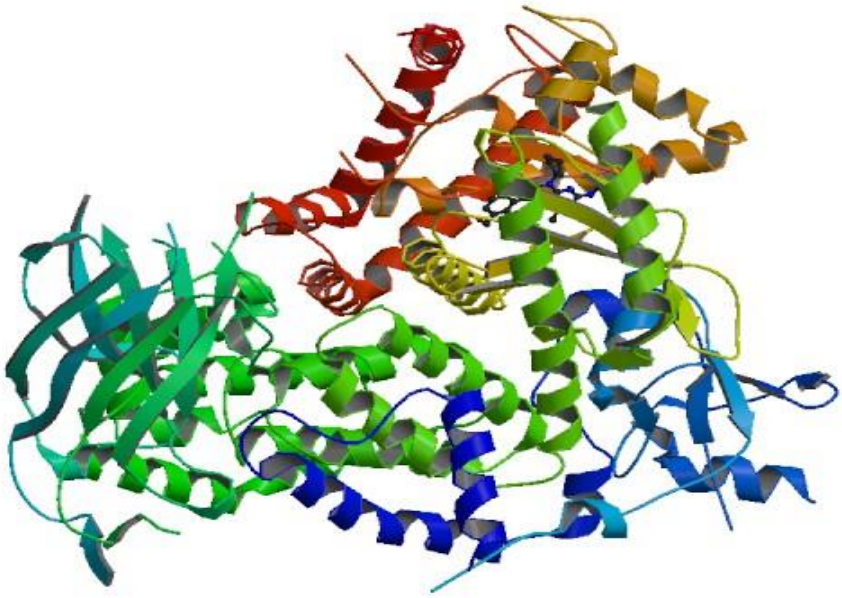

Figure 2. 3Ml8 Receptor

Table 1. Andrographolide analogous

S. No	Compounds	R	R_1	R_2	R_3
1.	5a	F	OH	H	H
2.	5b	F	SH	H	H
3.	5c	F	CH_3	H	H
4.	5d	F	OCH_3	H	H
5.	5e	F	OC_2H_5	H	H
6.	5f	F	NO_2	H	H
7.	5g	F	H	Cl	H
8.	5h	F	H	Br	H
9.	5i	F	H	$COCH_3$	H
10.	5j	F	H	CF_3	H
11.	5k	F	H	H	OH
12.	5l	F	H	H	SH
13.	5m	F	H	H	CH_3
14.	5n	F	H	H	OCH_3
15.	5o	F	H	H	OC_2H_5
16.	5p	F	H	H	NO_2
17.	5q	F	OCH_3	H	NO_2
18.	5r	F	NO_2	H	OCH_3

Table 2. ADME Analysis

Title	mol MW	QPlogPo/w	QPlogS	QPlogHERG	QPPCaco	QPlogBB	QPPMDCK	Percent Human Oral Absorption
1	659.79	5.306	-6.23	-5.725	104.72	-2.23	78.11	68.25
2	675.85	6.611	-8.101	-6.652	271.34	-1.839	496.44	83.29
3	657.82	5.911	-5.817	-4.904	393.34	-1.464	312.30	82.07
4	673.82	6.099	-6.2	-5.477	351.93	-1.651	273.04	82.31
5	687.80	6.954	-8.346	-7.042	307.69	-2.062	250.42	86.27
6	688.79	5.203	-4.517	-4.448	193.55	-1.682	144.83	59.46
7	678.24	7.032	-9.412	-7.306	165.65	-2.192	316.14	81.91
8	722.69	7.079	-9.463	-7.274	160.85	-2.191	329.25	81.97
9	685.83	5.22	-5.383	-5.137	196.37	-1.851	154.10	72.63
10	711.79	7.523	-9.113	-6.674	533.56	-1.352	1943.13	93.88
11	659.79	5.867	-8.586	-7.313	51.59	-3.076	36.34	66.03
12	675.85	6.837	-9.309	-7.363	165.00	-2.269	339.58	80.74
13	657.82	6.902	-9.379	-7.332	172.77	-2.377	134.19	81.49
14	673.82	6.428	-7.797	-6.54	248.72	-2.043	198.96	81.54
15	687.8	6.55	-7.966	-6.689	209.75	-2.284	126.12	80.93
16	688.79	5.859	-8.901	-7.333	20.45	-3.647	13.36	45.83
17	718.82	5.692	-8.019	-6.521	25.53	-3.386	16.62	46.58
18	718.82	5.548	-5.457	-5.31	268.38	-1.839	169.40	64.02
Standard range	<750	>5.0	<-6.5	< 5	<25-poor, >500-great	<-3.0	<25-poor, >500-great	<25% poor

Table 3. Docked scores of Andrographolide analogous

Compound's	Dock Score 3ML8	Bind with Amino Acid	H-Bonding
1	-4.12	**LYS 890, TYR 867,** ALA 885, VAL 882,	1.82, 1.88
2	-1.42	**TRP 812,** LYS 883, ALA 805, LYS 902	1.82, 1.85, 2.08
3	-5.44	LYS 802, ALA 805, ASP 964	1.99, 2.01, 1.89
4	-5.00	LYS 883, ASP 964, LYS 902	1.92, 1.95, 1.93
5	-5.42	**TYR 831,** LYS 883, LYS 802	1.80, 2.08
6	-4.65	SER 802, LYS 807, VAL 882, ALA 805, LYS 802	1.90, 2.04, 2.54
7	-4.21	VAL 882, LYS 833, ASP 964, LYS 890	1.87, 2.09, 2.22
8	-2.92	ASP 950, LYS 807, LYS 802, LYS 890	1.88, 2.03
9	-7.23	VAL 882, ASP 950, LYS 807, LYS 802	1.88, 2.17, 2.53
10	-2.98	VAL 882, ALA 805	2.37, 2.43
11	-7.35	ASP 841, ASP 950	2.07, 2.44
12	-4.09	LYS 802,	1.95, 2.62
13	-5.91	-	-
14	-7.40	LYS 802, ASP 964	1.99
15	-3.26	ALA 805, ASP 950	1.69, 2.22
16	5.91	LYS 890	2.08, 2.26
17	-5.97	-	2.53
18	-4.87	ASP 950	1.65
Doxorubicin	-7.72	LYS 802, VAL 882	1.68

Table 4. MTT Assay of Andrographolide analogous

S.No	HePG2	MCF-7	HCT116	PC3
1	47.52±1.32	36.32±0.43	38.46±0.31	41.74±1.15
2	24.12±0.16	19.18±1.09	25.42±0.26	29.64±1.03
3	51.23±1.13	41.72±1.76	46.16±1.17	45.16±0.93
4	52.10±0.46	42.53±1.62	47.76±0.19	46.27±0.92
5	48.46±1.02	37.14±0.12	39.16±0.23	42.64±1.05
6	28.06±1.13	18.26±0.42	26.13±0.52	28.12±1.24
7	48.02±1.05	36.83±0.13	39.61±1.15	42.01±1.21
8	41.17±0.12	30.46±.0.12	29.92±0.14	32.02±1.16
9	16.16±0.53	17.03±1.17	17.79±1.02	19.82±0.12
10	46.21±0.13	34.07±1.47	36.72±1.10	39.46±0.32
11	11.24±1.08	9.21±1.05	8.09±1.24	13.21±1.06
12	50.52±0.52	41.30±1.34	42.82±1.72	44.14±1.35
13	22.64±1.62	13.71±1.06	14.04±1.13	23.26±1.21
14	8.13±1.02	7.18±1.22	6.24±0.84	10.06±1.02
15	49.96±0.32	39.34±0.72	42.62±1.14	43.74±1.17
16	56.18±1.16	44.38±1.02	49.16±1.98	51.25±1.26
17	49.22±1.72	38.16±0.33	39.46±1.12	43.40±1.02
18	34.12±0.25	27.83±0.82	26.02±1.05	31.23±1.52
Doxorubicin	**4.52 ±1.12**	**4.03± 1.05**	**5.26± 0.96**	**8.24± 1.26**

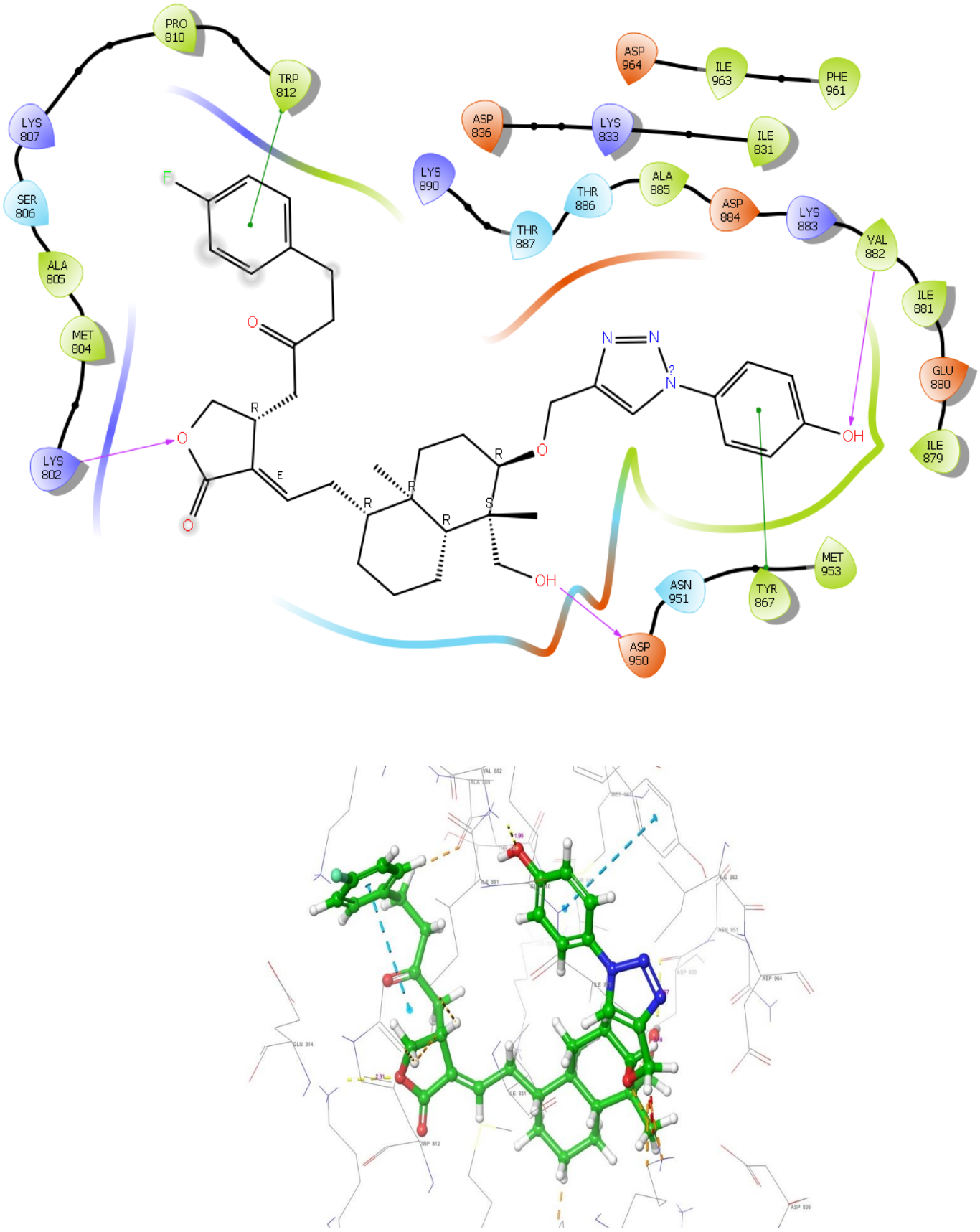

Figures 3. Compound 11, 2D & 3D Ligand Protein Interactions

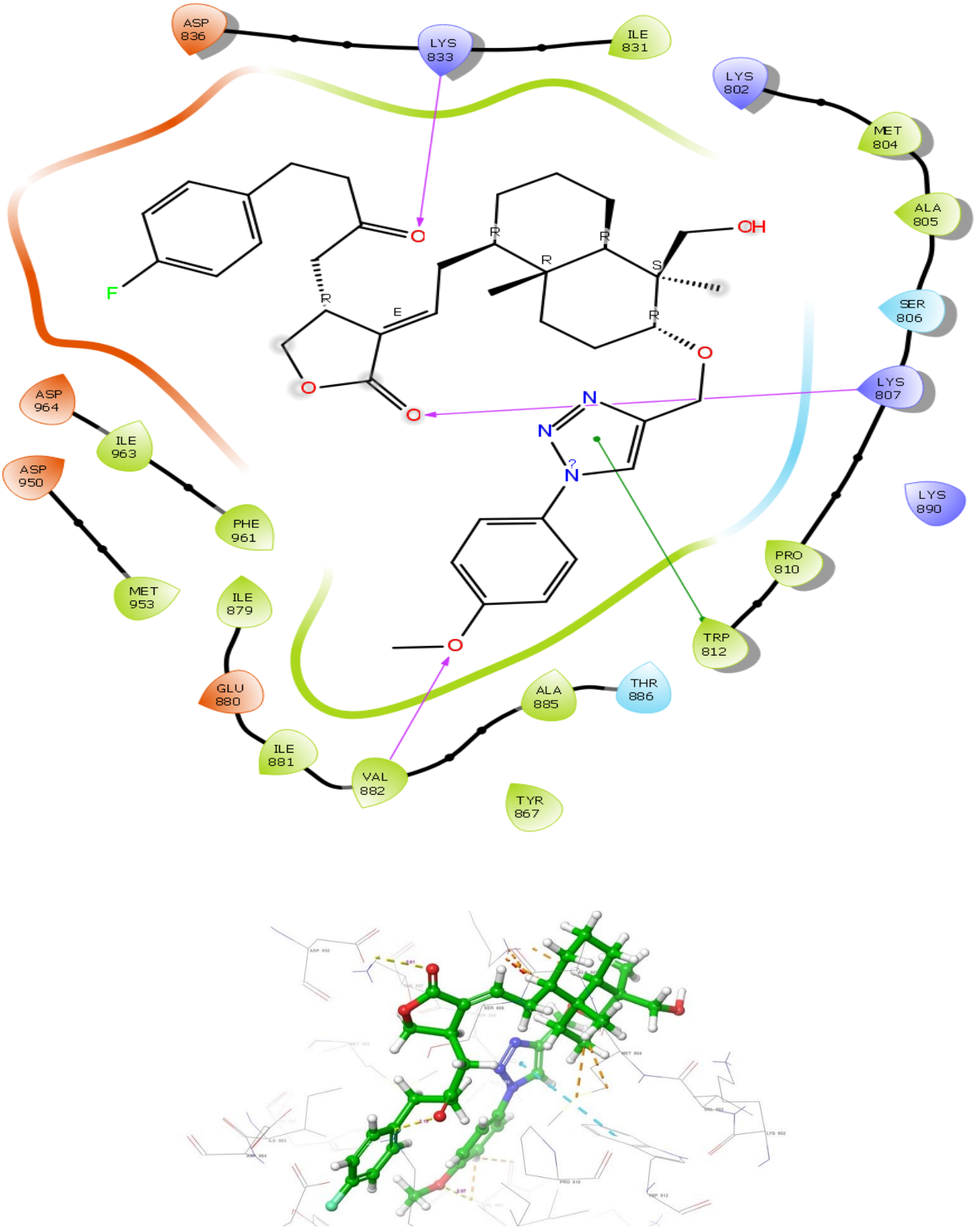

Figures 4. Compound 14, 2D & 3D Ligand Protein Interactions

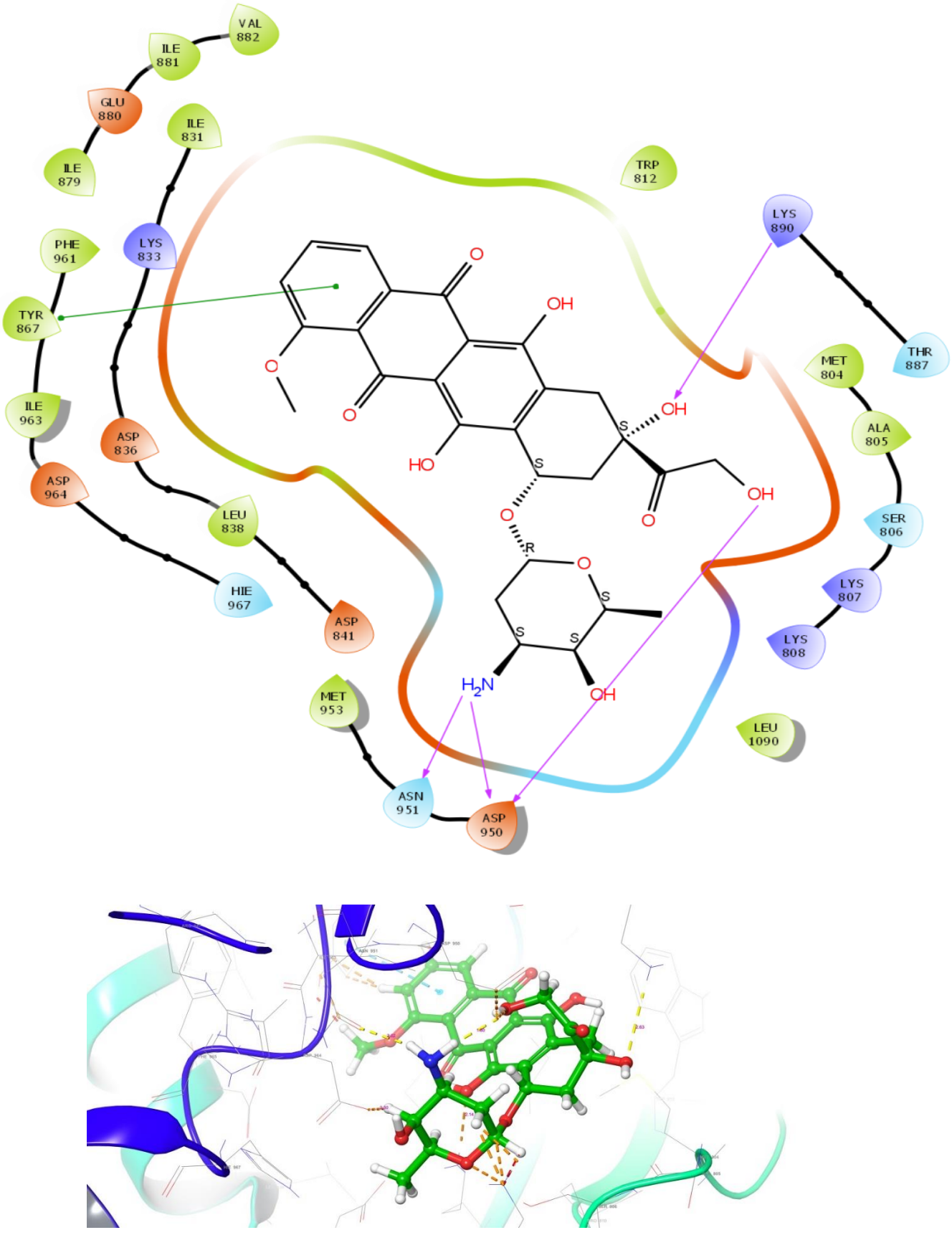

Figures 5. Doxorubicin 2D & 3D Ligand Protein Interactions

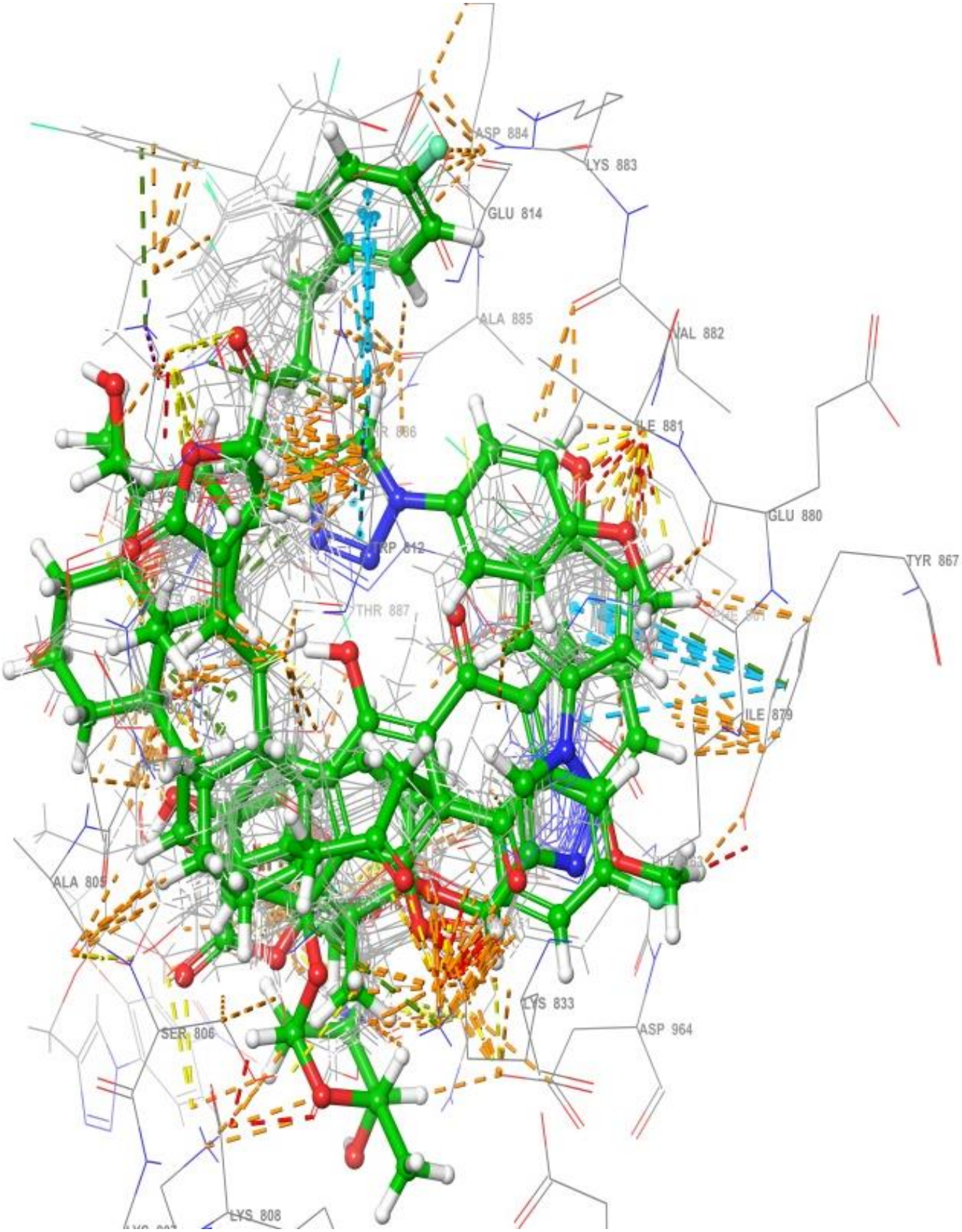

Figures 6. All Compounds Docking Poses

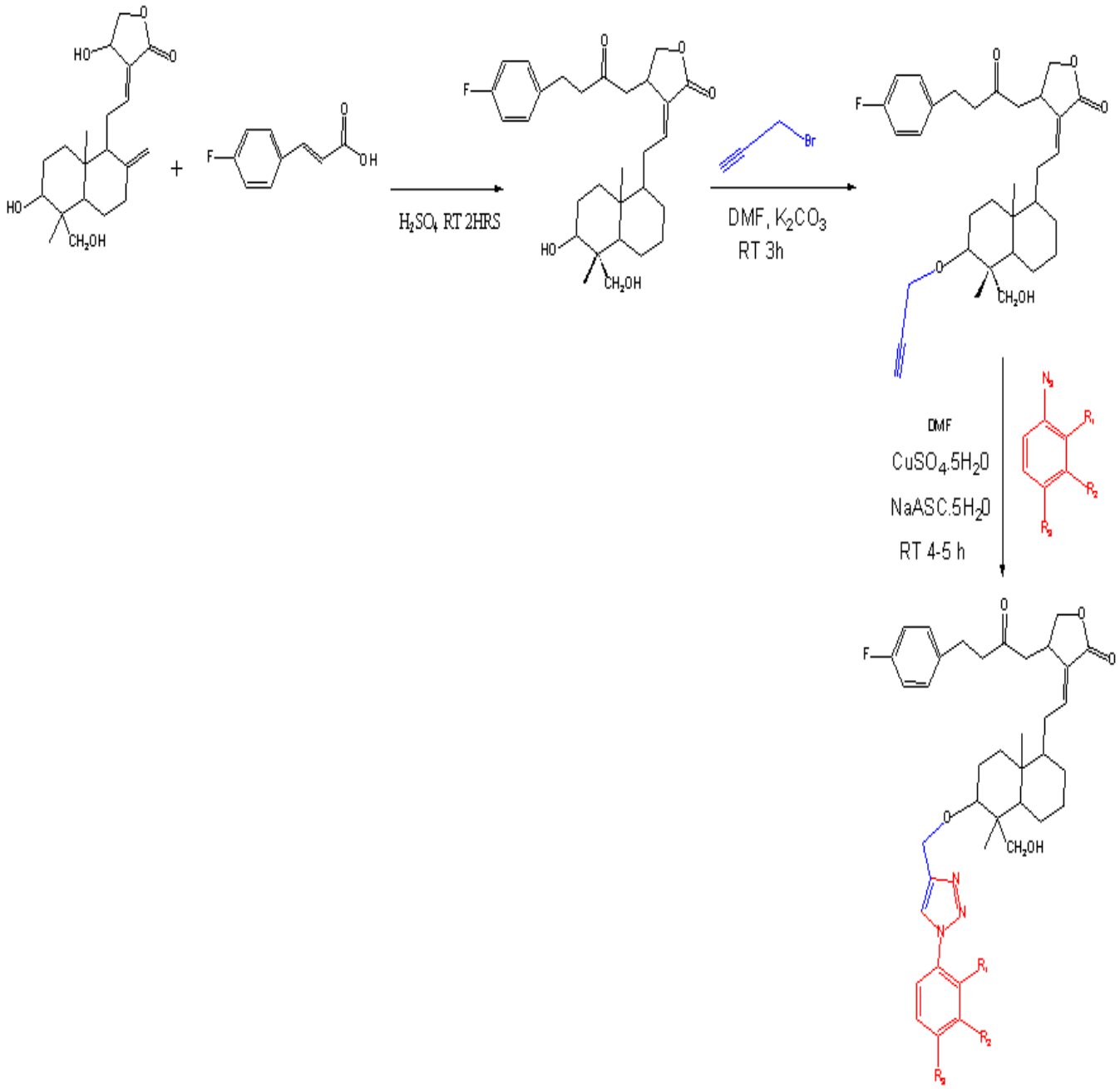

Figure 7. General Synthetic scheme of new Andrographolides

Each ligand was individually docked using the prepared 3D structures. Prior to docking, the receptor protein structure 3ML8 (discovered as the highly potent PI3K/mTOR inhibitor PF-04691502 through SBDD) was prepared. Heteroatoms and water molecules were removed from the 3ML8 PDB file. PI3K, AKT, and mTOR are key kinases within the PI3K pathway, with phosphoinositide 3-kinase α (PI3Kα) playing a crucial role in various cancers. The receptor grid was generated using the Glide module to define the docking region on the protein. Molecular docking studies were conducted using the Maestro module of the Schrödinger 11.4 suite of automated docking systems. This allowed for the prediction of ligand affinity, quantitative structure-activity relationship (QSAR) analysis, assessment of absorption, distribution, metabolism, excretion, and toxicity (ADMET), as well as determination of the binding orientation of the ligands to the target protein. The interactions between the 3ML8 protein and the ligand conformations were investigated, including hydrogen bond angles, energy, and bond lengths. Among the 18 analogues tested, compounds 14, 11, and 9 exhibited the most potent binding interactions with the PI3K inhibitor. Compound 14 was found to bind with amino acids LYS 802 and ASP 964, forming hydrogen bonds with bond lengths of 1.99 Å. Compound 11 interacted with amino acids ASP 841 and ASP 950, with hydrogen bond lengths of 2.07 Å and 2.44 Å, respectively. Compound 9 showed binding interactions with amino acids VAL 882, ASP 950, LYS 807, and LYS 802, forming hydrogen bonds with bond lengths of 1.88 Å, 2.17 Å, and 2.53 Å. These findings suggest that compounds 14, 11, and 9 exhibit strong potential as PI3K inhibitors, with favorable binding affinities and interactions with key amino acids within the binding pocket of the target protein. Table 3. Docking studies of all 18 compounds against PI3K protein, best potent molecules were evaluated based on the binding energy and docking energy (kcal/mol). Based on the docking score, the best potent compounds identified. Figure-3.

3.3. Cytotoxic Activity

Cytotoxic activity of andrographolide analogous to human cancer cells. The human liver carcinoma cell line (HePG-2), the human breast cancer cell line (MCF-7), the human colon carcinoma cell line (HCT-116), and the human prostate cancer cell line (PC3) were used to establish the inhibitory concentration (IC_{50}), It is a measure of a substance's ability to inhibit a specific biological process of 18 andrographolide compounds on cell growth using MTT assay. Table 4. The primary objective of this research article is to comprehensively assess the pharmacological potential of 18 andrographolide analogues, with a specific focus on their suitability as potential drug candidates for cancer treatment. Through a rigorous analysis encompassing Lipinski's Rule of Five and pharmacokinetic parameters such as molecular weight, partition coefficient, and water solubility, we aim to elucidate the compounds' drug-like behavior and oral bioavailability. Furthermore, molecular docking studies against the PI3K protein provide crucial insights into the compounds' binding affinities and potential as inhibitors of this key kinase involved in cancer signaling pathways. Additionally, the evaluation of cytotoxic activity against various human cancer cell lines serves to identify compounds with promising anticancer properties. By addressing these objectives, this research contributes valuable knowledge to the field of drug discovery, potentially paving the way for the development of novel andrographolide-based therapeutics for cancer treatment [22-32].

4. Conclusions

In conclusion, our study investigated that the ADME prediction properties results were selected for docking studies for PI3K inhibitor. The exactly fit into the 3ML8 protein active site region, ligand formed H-bond interactions to the receptor. Therefore, *in-silico* studies states the importance of ligand and their protein interaction. SAR suggested that the compounds 14, 11, and 9 are more potent molecules when compared with other andrographolide compounds. The ligand-protein interactions play a very important role in structural-based drug designing (SBDD). The approach utilized in this docking study results is successful in evaluating novel PI3K inhibitors. The ligands 14 (-7.40), 11 (-7.35), and 9(-7.23), showed high binding affinity against PI3K Inhibitor compared to the standard drug doxorubicin (-7.72). The cytotoxic effects of various andrographolide analogues against multiple human cancer cell lines, including HepG2, MCF-7, HCT116, and PC3. Through the evaluation of inhibitory concentration (IC50) values, we identified compounds 14, 11, and 9 as the most potent cytotoxic molecules across all tested cell lines. These findings suggest that structural modifications to andrographolide can significantly enhance its anticancer activity. Further studies are warranted to elucidate the underlying mechanisms of action of these compounds and their potential as therapeutic agents for the treatment of human cancers. Additionally, preclinical studies are needed to assess their efficacy and safety profiles before clinical translation. Overall, our results contribute to the growing body of evidence supporting the development of andrographolide derivatives as promising candidates for cancer therapy.

Conflicts of Interest

All authors declare that they have no competing interests.

Acknowledgments

The authors are heartily grateful to the Dean of Pharmacy, Principal- University College of Technology, Osmania University, Hyderabad and One of the authors is thankful to ICMR No.3/2/2/56/2018/Online Onco Fship/NCD-III for providing support. Schrodinger software, USA .and VIPER providing anticancer screening facilities.

References

[1] D. Chakraborty, R.N. Chakravarti. (1952). Andrographolide. Part-1. J Chem Soc. 314 1697-1700.

[2] J. Zhou, S. Zhang, O. Choon-Nam, H.M. Shen. (2006). Critical role of pro-apoptotic Bcl-2 family members in andrographolide-induced apoptosis in human cancer cells. Biochemical pharmacology. 72 (2) 132-144.

[3] J.X. Chen, H.J. Xue, W.C. Ye, B.H. Fang, Y.H. Liu, S.H. Yuan, Y.Q. Wang. (2009). Activity of

andrographolide and its derivatives against influenza virus in vivo and in vitro. Biological and Pharmaceutical Bulletin. 32 (8) 1385-1391.

[4] V. Yerragunta, K. Waghray, N.J.P. Subhashini. (2021). Anti-Cancer Activity of Andrographolide: A Review. Journal of Pharmaceutical Research International. 33 (43B) 1-9.

[5] S. Rajagopal, R.A. Kumar, D.S. Deevi, C. Satyanarayana, R. Rajagopalan. (2003). Andrographolide, a potential cancer therapeutic agent isolated from Andrographis paniculata. Journal of Experimental therapeutics and Oncology. 3 (3) 147-158.

[6] A.K. Thakur, S.S. Chatterjee, V. Kumar. (2015). Adaptogenic potential of andrographolide: An active principle of the king of bitters (Andrographis paniculata). Journal of Traditional and Complementary Medicine. 5 (1) 42-50.

[7] V. Yerragunta, W. Kavita D.A. Shivraj. (2023). Molecular Docking Studies of Novel Andrographolide analogs using Phosphoinositide 3-kinase (PI3K) as a potent anti-cancer inhibitor Eur. Chem. Bull. 12 (Special Issue 4) 19594–19607.

[8] T. Jayakumar, C.Y. Hsieh, J.J. Lee, J.R. Sheu. (2013). Experimental and clinical pharmacology of Andrographis paniculata and its major bioactive phytoconstituent andrographolide. Evidence-Based Complementary and Alternative Medicine, 2013.

[9] A.K. Thakur, S.S. Chatterjee, V. Kumar. (2015). Adaptogenic potential of andrographolide: An active principle of the king of bitters (Andrographis paniculata). Journal of Traditional and Complementary Medicine. 5 (1) 42-50.

[10] A.E. Nugroho, M. Andrie, N.K. Warditiani, E. Siswanto, S. Pramono, E. Lukitaningsih. (2012). Antidiabetic and antihiperlipidemic effect of Andrographis paniculata (Burm. f.) Nees and andrographolide in high-fructose-fat-fed rats. Indian journal of pharmacology. 44 (3) 377-381.

[11] J. Bajorath, T.E. Klein, T.P. Lybrand, J. Novotny. (1999). Computer-aided drug discovery: From target proteins to drug candidates. In Biocomputing'99. 413-414.

[12] C. Aromdee. (2014). Andrographolide: progression in its modifications and applications–a patent review (2012–2014). Expert Opinion on Therapeutic Patents. 24 (10) 1129-1138.

[13] Z. Zhai, X. Qu, H. Li, Z. Ouyang, W. Yan, G. Liu, A. Qin. (2015). Inhibition of MDA-MB-231 breast cancer cell migration and invasion activity by andrographolide via suppression of nuclear factor-κB-dependent matrix metalloproteinase-9 expression Corrigendum in/10.3892/mmr. 2019.9833. Molecular medicine reports. 11 (2) 1139-1145.

[14] M. Banerjee, S. Chattopadhyay, T. Choudhuri, R. Bera, S. Kumar, B. Chakraborty, S.K. Mukherjee. (2016). Cytotoxicity and cell cycle arrest induced by andrographolide lead to programmed cell death of MDA-MB-231 breast cancer cell line. Journal of biomedical science. 23 1-17.

[15] S.R. Johnston. (2010). New strategies in estrogen receptor–positive breast cancer. Clinical Cancer Research. 16 (7) 1979-1987.

[16] S. Rossi, C. Sevignani, S.C. Nnadi, L.D. Siracusa, G.A. Calin. (2008). Cancer-associated genomic regions (CAGRs) and noncoding RNAs: bioinformatics and therapeutic implications. Mammalian Genome. 19 (7) 526-540.

[17] G.P. George, R.D. Mittal. (2010). MicroRNAs: Potential biomarkers in cancer. Indian Journal of Clinical Biochemistry. 25 4-14.

[18] F.M. Badr. (2016). Potential role of miR-21 in breast cancer diagnosis and therapy. SciMed Central. 3 (5) 1068-75.

[19] S.L. Anwar, D.N.I. Sari, A.I. Kartika, M.S. Fitria, D.S. Tanjung, D. Rakhmina, T. Aryandono. (2019). Upregulation of circulating MiR-21 expression as a potential biomarker for therapeutic monitoring and clinical outcome in breast cancer. Asian Pacific Journal of Cancer Prevention: APJCP. 20 (4) 1223.

[20] H. Go, J.Y. Jang, P.J. Kim, Y.G. Kim, S.J. Nam, J.H. Paik, Y.K. Jeon. (2015). MicroRNA-21 plays an oncogenic role by targeting FOXO1 and activating the PI3K/AKT pathway in diffuse large B-cell lymphoma. Oncotarget. 6 (17) 15035.

[21] F. Luongo, F. Colonna, F. Calapà, S. Vitale, M.E. Fiori, R. De Maria. (2019). PTEN tumor-suppressor: the dam of stemness in cancer. Cancers. 11 (8) 1076.

[22] C. Zhang, K. Liu, T. Li, J. Fang, Y. Ding, L. Sun, X. Sun. (2016). miR-21: A gene of dual regulation in breast cancer. International journal of oncology. 48 (1) 161-172.

[23] R.A. Kumar, K. Sridevi, N.V. Kumar, S. Nanduri, S. Rajagopal. (2004). Anticancer and immunostimulatory compounds from Andrographis paniculata. Journal of ethnopharmacology. 92 (2-3) 291-295.

[24] S. Harjotaruno, A. Widyawaruyanti, S. Sismindari, N.C. Zaini. (2007). Apoptosis inducing effect of andrographolide on TF-47 human breast cancer cell line. African Journal of Traditional, Complementary and Alternative Medicines. 4 (3) 345-351.

[25] H.L. Soo, S.Y. Quah, I. Sulaiman, S.R. Sagineedu, J.C.W. Lim, J. Stanslas. (2019). Advances and challenges in developing andrographolide and its analogues as cancer therapeutic agents. Drug discovery today. 24 (9) 1890-1898.

[26] D. Weber, M. Zhang, P. Zhuang, Y. Zhang, J. Wheat, G. Currie. (2017). The efficacy of andrographolide and its combination with betulinic acid in the treatment of triple-negative breast cancer. Cancer Therapy & Oncology International Journal. 4 (1) 1-10.

[27] C. Agatemor, S.A.D. Middleton, D. Toledo. (2022). How pervasive are post-translational and-transcriptional modifications?. Trends in cell biology. 32 (6) 475-478.

[28] A.M. Stark, S. Pfannenschmidt, H. Tscheslog, N. Maass, F. Rösel, H.M. Mehdorn, J. Held-Feindt. (2006). Reduced mRNA and protein expression of BCL-2 versus decreased mRNA and increased protein expression of BAX in breast cancer brain metastases: a real-time PCR and

immunohistochemical evaluation. Neurological research. 28 (8) 787-793.

[29] G. Ichim, S.W. Tait. (2016). A fate worse than death: apoptosis as an oncogenic process. Nature Reviews Cancer/ 16 (8) 539-548.

[30] J.Y. Kim, J.H. Park. (2003). ROS-dependent caspase-9 activation in hypoxic cell death. FEBS letters. 549 (1-3) 94-98.

[31] G.J. Zhang, I. Kimijima, M. Onda, M. Kanno, H. Sato, T. Watanabe, S. Takenoshita. (1999). Tamoxifen-induced apoptosis in breast cancer cells relates to down-regulation of bcl-2, but not bax and bcl-XL, without alteration of p53 protein levels. Clinical Cancer Research. 5 (10) 2971-2977.

[32] S.J. Humphrey, G. Yang, P. Yang, D.J. Fazakerley, J. Stöckli, J.Y. Yang, D.E. James. (2013). Dynamic adipocyte phosphoproteome reveals that Akt directly regulates mTORC2. Cell metabolism. 17 (6) 1009-1020.